International Journal of Remote Sensing
Vol. 29, No. 3, 10 February 2008, 767–786

Taylor & Francis
Taylor & Francis Group

Estimation of chlorophyll-*a* concentration and trophic states for inland lakes in Northeast China from Landsat TM data and field spectral measurements

H. DUAN†‡, Y. ZHANG*§, B. ZHANG†, K. SONG†, Z. WANG†, D. LIU† and F. LI†‡

†Northeast Institute of Geography and Agricultural Ecology, Chinese Academy of Sciences, Changchun 130012, China

‡Graduate School of Chinese Academy of Sciences, Beijing 100039, China

§Institute of Space and Earth Information Science, The Chinese University of Hong Kong, Shatin, NT, Hong Kong

(*Received 6 April 2006; in revised form 14 March 2007*)

Landsat TM data and field spectral measurements were used to evaluate chlorophyll-*a* (Chl-*a*) concentration levels and trophic states for three inland lakes in Northeast China. Chl-*a* levels were estimated applying regression analysis in the study. The results obtained from the field reflectance spectra indicate that the ratio between the reflectance peak at 700 nm and the reflectance minimum at 670 nm provides a relatively stable correlation with Chl-*a* concentration. Their determination of coefficients R^2 is 0.69 for three lakes in the area. From Landsat TM data, the results show that the most successful Chl-*a* was estimated from TM3/TM2 with $R^2=0.63$ for the two lakes on 26 July 2004, from TM4/TM3 with $R^2=0.89$ for the two lakes on 14 October 2004, and from the average of TM2, TM3 and TM4 with $R^2=0.72$ for the three lakes tested on 13 July 2005. These results are applicable to estimate Chl-*a* from satellite-based observations in the area. We also evaluate the trophic states of the three lakes in the region by employing Shu's modified trophic state index (TSI_M) for the Chinese lakes' eutrophication assessment. Our study presents the TSI_M from different TM data with R^2 more than 0.73. The study shows that satellite observations are effectively applied to estimate Chl-*a* levels and trophic states for inland lakes in the area.

1. Introduction

Lakes are valuable water resources and can be used for fishing, transport, agriculture, industry, recreation and tourism. To date, water quality conditions for numerous lakes around the world are so badly deteriorated that they are hardly recoverable by natural means of purification. The most common ecological problem of inland water bodies is the anthropogenic eutrophication. Since the change of water environment typically results from economic development and sewage treatment, it has become the most widespread water quality problem in China and many other countries as well (e.g., Giardino *et al.* 2001, Chen *et al.* 2004, Wang *et al.* 2004). For this reason, water quality deterioration and eutrophication issues have been paid more and more attention by the public and government, and many

*Corresponding author. Email: yuanzhizhang@cuhk.edu.hk

International Journal of Remote Sensing
ISSN 0143-1161 print/ISSN 1366-5901 online © 2008 Taylor & Francis
http://www.tandf.co.uk/journals
DOI: 10.1080/01431160701355249

studies have been carried out to evaluate the water trophic state for inland lakes (e.g., Dekker and Peters 1993, Xing *et al.* 2005).

Chlorophyll-*a* (Chl-*a*) is a key parameter to determine the trophic state index and one of the major factors affecting water environment, which produces visible changes in the surface of waters (Ritchie *et al.* 1990, Zhang *et al.* 2002, 2003a, 2003b). Since Chl-*a* exists in all algae groups in marine and freshwater systems, Chl-*a* concentration is an important indicator for the bio-production of inland water bodies (Brivio *et al.* 2001, Ostlunda *et al.* 2001).

The trophic state index is an important parameter to assess water quality conditions. Walker (1979) proposed a 0–100 scale of continuous numerical classification for lake's trophic states and a rigorous base on quantitative studies of the mechanism behind eutrophication issues (Porcella *et al.* 1980, Aizaki *et al.* 1981). The method eliminates the subjective labels associated with the use of such oligotrophic, mesotrophic and eutrophic states as its indicators (Xu *et al.* 2001). Carlson (1977) suggested one of the most suitable and acceptable methods for evaluating inland lake's eutrophication. Carlson's method provides an approach to define a trophic state and determine it for inland lakes. A numerical trophic state index is incorporated into a scale of 0–100. Each major division (e.g., 10, 20, 30 etc.) represents a doubling in algal biomass. The index can be calculated from one of several parameters such as Chl-*a*, Secchi disk depth and total phosphorus. However, for various geographic sites, environmental issues and human activities, the type of a lake's eutrophication and its assessment methods are different. This difference requires researchers looking for a more suitable method to evaluate the Chinese lakes' status of eutrophication. Shu (1990, 1993) investigated 24 Chinese representative lakes and proposed a modified method fitting for Chinese lake eutrophication assessment. In Shu's method, chlorophyll-*a* was employed to calculate the trophic state index for lakes.

Space-borne observations can provide a suitable means to integrate limnological data collected from traditional measurements (Giardino *et al.* 2001). However, satellite measurements cannot be independently analysed and applied using specific absorption characteristics without supporting reference data. Therefore, the additional use of *in situ* samples and field reference spectra can assist in finding new methods and improving the accuracy of estimation (Thiemann and Kaufmann 2000, Erkkila and Kalliola 2004).

This study presents the application of Landsat TM and field spectral measurements to the estimation of Chl-*a* concentration and the trophic state index for three lakes in the northwest Jilin Province in Northeast China. The trophic state index (TSI_M) modified by Shu (1990, 1993) was applied to evaluate the trophic status of the three lakes in the study. Our data analyses were also supported with additional ground truth reference data and field spectral measurements taken from a boat-borne platform.

2. Study area and materials

2.1 *Study area*

The study area of three lakes is located in the northwest Jilin Province of Northeast China. The surface lake area covers about 416 km^2, including Lake Chagan, Lake Xinmiao and Lake Kuli (see figure 1). Lake Kuli is isolated from the other two

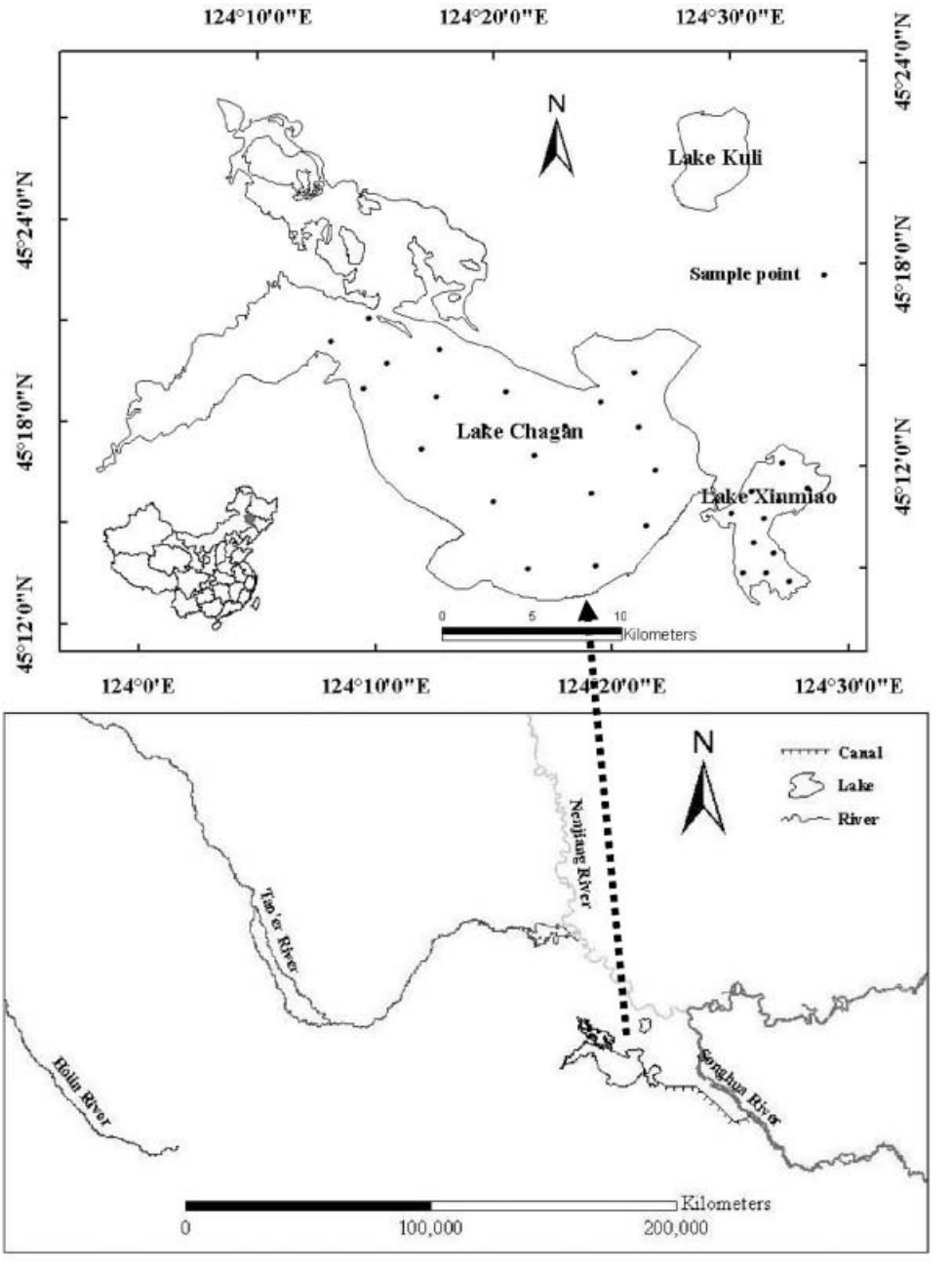

Figure 1. Location of the Chagan Lake region in China.

lakes, while Lake Chagan and Lake Xinmiao are interconnected to each other by a canal.

Lake Chagan is one of the 10 largest freshwater lakes in China. It has a mean surface area of 372 km^2, a mean depth of 2.52 m, and the largest storage capacity of 5.98×10^8 m^3. Lake Xinmiao has a mean surface area of 31 km^2, a mean depth of

Table 1. Sample number, Chl-*a* contents and Secchi disk depth in Lake Chagan.

	May	June	July	August	September	October
Sample number	11	6	8	9	20	20
Chl-*a* (μg/L)						
min	6.34	6.40	28.14	15.15	11.24	10.68
max	19.13	14.68	58.21	37.15	47.23	28.68
mean	14.26	10.22	40.57	28.81	24.38	20.91
SDT (m)						
min	0.09	0.10	0.22	0.22	0.18	0.10
max	0.30	0.46	0.24	0.30	0.32	0.27
mean	0.14	0.25	0.23	0.25	0.25	0.14

15 m, and a storage capacity of $5.1 \times 10^7\,m^3$, while Lake Kuli has a mean surface area of $13\,km^2$, a mean depth of 2 m, and a storage capacity of $2.5 \times 10^7\,m^3$.

Since Songhua River first flows into Lake Xinmiao through a canal and then runs out of Lake Chagan, the Songhua River is the main source of the lakes region. Its tributaries such as the Holin River, Tao'er River and Nenjiang River are the secondary supplies of the lakes. Other water supplies include natural precipitation and ground water. In addition, the lakes' primary economic value is fishery, but it is also important for agriculture and recreational uses. Therefore, a long-term observation of water quality monitoring programme for lake conservation is still needed.

2.2 *Water sampling and measurements*

Water sampling and measurements were performed in 2004 and 2005, respectively. Our fieldwork was carried out monthly from May to October 2004 and also in 2005 several times. The monitoring frequency was once a month. All water sampling and fieldwork was conducted in Lake Chagan and Lake Xinmiao, but not including Lake Kuli. However, we collected some data from Lake Kuli in July 2005 from the local monitoring stations for the purpose of comparing with our estimated results. Due to the availability of water sample analysis in the laboratory, the number of water samples in different months varied from 6 to 20 for Lake Chagan (table 1), and from 3 to 11 for Lake Xinmiao (table 2). In early July 2005, an extra session of fieldwork was carried out in Lake Chagan. In each fieldwork, the position of the sampling boat was geo-located by a portable Ashtech ProMark2 Global Position System (GPS) receiver with 0.3–3 m accuracy specification. SDT and field spectral

Table 2. Sample number, Chl-*a* contents and Secchi disk depth in Lake Xinmiao.

	May	June	July	August	September	October
Sample number	9	5	7	3	4	11
Chl-*a* (μg/L)						
Min	0.35	4.01	4.76	22.87	12.16	6.23
Max	1.29	26.96	44.48	27.45	24.28	11.08
Mean	0.84	16.62	28.58	24.53	17.12	8.61
SDT (m)						
Min	—	0.60	0.23	0.26	0.30	0.38
Max	—	0.96	0.79	0.30	0.37	0.55
Mean	—	0.70	0.46	0.28	0.35	0.47

data were simultaneously measured at selected points of the lakes. At each sampling site, the lake water was also collected with a clean bottle for further laboratory analysis within four hours. Water quality parameters chosen for *in situ* measurements included physical (e.g., SDT, turbidity, and total suspended matter) and chemical measurements (e.g., Chl-*a*, pH, TN, TP) (Zhang *et al*. 2003c). However, Chl-*a* concentration was only analysed and assessed in the study.

Water samples were analysed in the laboratory within 2–4 hours after water sampling. A water sample was filtered using a glass micro-fibre filter (0.45 μm) to measure Chl-*a* with the standard spectro-photometric method. Acetone was used to extract Chl-*a* from the water sample for over 24 hours. The sample was then read before and after its acidification using a spectro-photofluorometer. Finally, Chl-*a* was calculated by comparison with the known standards (Schalles *et al*. 1998, Ahn *et al*. 2006).

2.3 *Field spectral measurements*

Field spectral measurements and acquisition of *in situ* data were conducted in selected test-sites. Field spectra were measured with a portable Analytical Spectral Devices (ASD) spectroradiometer (http://www.asdi.com/). The ASD radiometer has a spectral range between 350 and 1100 nm and a radiometric resolution of about 3 nm. The measurements were taken from the boat-borne platform above the lake surface at about 1 m in the vertical downward direction. Each measured position was oriented to the boat side within the light propagation to minimize the sun-glint from waves, but far away from the effect of the boat's shadow.

2.4 *Landsat TM data*

During concurrent in situ water measurements, cloud-free Landsat TM images in the same days of our fieldwork were also selected for the data analysis. This selection criterion significantly reduced the pool of TM images suitable for the analysis. We found three dates of Landsat TM data available for our study and in line with the criterion. Three scenes of Landsat TM data were acquired on 26 July 2004, 14 October 2004 and 13 July 2005, respectively. In each date of these three TM data, the weather condition was good enough with the wind speed less than 5 m/s and without cloud cover in the study area.

3. Methods

3.1 *Geometric correction*

For the TM data geo-coding, one TM image was first geometrically corrected using ground control points (GCPs) with ENVI software. 10 GCP were acquired by the GPS receiver to rectify the TM image of the three lake's areas. The TM image was also re-sampled using the nearest neighbour method to preserve its radiometry. The other two TM images were geo-coded to that TM scene as their master image.

3.2 *Atmospheric correction*

Atmospheric correction was performed using the 6S (Second Simulation of Satellite Signal in the Solar Spectrum) model (Lee and Kaufman 1986; Ghulam *et al*. 2004). This model corrects at-sensor radiance images for solar illuminance, Rayleigh and aerosol scattering. The input to the 6S specifies geometrical, spectral, and

Table 3. Regressive equations and relation coefficients indicating the relationship between Chl-*a* content and spectral reflectance ratios in Lake Chagan.

Band ratio	Regressive equation	R^2	Band ratio	Regressive equation	R^2
710/440	y=42.805x–41.959	0.20	810/670	y=44.677x–6.539	0.19
710/670	y=78.018x–65.88	0.64	750/670	y=42.154x–1.041	0.15
700/670	y=93.67x–90.40	0.69	560/440	y=27.386x–26.903	0.14
710/680	y=74.782x–64.065	0.62	700/680	y=88.274x–86.206	0.67

Note: x means the band ratio, and y refers to Chl-*a*.

atmospheric and target conditions. The visibility was obtained from local weather stations. Consequently, we used standard models for other atmospheric parameters. These models were chosen as mid-latitude summer and continental aerosol models. The choices were made, considering the general weather situation during the period of our collected data. We assumed the study area as a homogenous ground without directional effects. Other (non-atmospheric) inputs to the 6S were ground truth measured reflectance, latitude, longitude of the target lake, time of day and date of year. The ground truth reflectance made it possible for the code to simulate the radiance at the TM sensor altitude (Ostlunda *et al*. 2001). This radiance simulation was applied to all three scenes of TM data employed in the study. The method was used with the atmospheric correction of TM visible and near-infrared bands. Sensitivity analysis was also conducted by comparisons of corrected and uncorrected reflectance data, including spectral brightness.

3.3 *Relationship between Chl-a and spectral measurements*

The use of channel ratios for relationships between spectral measurements and ground truth data is quite common. The advantage of using ratios over absolute values of reflectance is that they correct some of the effects of measurements geometrically and atmospherically (e.g., Koponen *et al*. 2001, 2002, Pulliainen *et al*. 2001). The common Chl-*a* algorithm has been the reflectance ratio between two channels in the region of 670–720 nm (Kallio *et al*. 2001), which can enlarge their differences between the absorption maximum and the reflectance peak of Chl-*a*. Previous studies (Gitelson and Kondratyev 1991, Dekker 1993) proposed a good correlation between the ratio of the reflectance peak (705 nm) over the absorption maximum (675 nm) and Chl-*a* concentration.

In the study, previous Chl-*a* retrievals were examined empirically by deriving the regression algorithms for all possible band combinations, and selecting the one with the highest correlation coefficient or R^2. These algorithms and their parameters are given in tables 3–5. Our analyses with wavelength positions in the absorption

Table 4. Regressive equations and relation coefficients indicating the relationship between Chl-*a* content and spectral reflectance ratios in Lake Xinmiao.

Band ratio	Regressive equation	R^2	Band ratio	Regressive equation	R^2
710/440	y=37.53x–37.868	0.66	810/670	y=85.051x–26.865	0.61
710/670	y=67.325x–53.486	0.69	750/670	y=95.623x–26.289	0.51
700/670	y=71.366x–66.686	0.70	560/440	y=33.143x–50.424	0.28
710/680	y=73.886x–60.064	0.70	**700/680**	y=81.722x–78.453	0.72

Note: x means the band ratio, and y refers to Chl-*a*.

Table 5. Regressive equations and relation coefficients indicating the relationship between Chl-*a* content and spectral reflectance ratios in both lakes.

Band ratio	Regressive equation	R^2	Band ratio	Regressive equation	R^2
710/440	y=41.214x–40.738	0.42	810/670	y=54.771x–12.86	0.37
710/670	y=71.893x–58.605	0.68	750/670	y=57.019x–9.695	0.31
700/670	y=84.36x–79.93	0.70	560/440	y=20.642x–18.215	0.09
710/680	y=70.195x–57.858	0.67	**700/680**	y=85.427x–82.676	0.71

Note: x means the band ratio, and y refers to Chl-*a*.

maximum and reflectance peak resulted in almost the same relationships as reported studies (Gitelson *et al*. 1993, Arenz *et al*. 1996). However, the absorption maximum and reflectance peak positions have a small shift in our datasets.

Previous studies suggest that the logarithmic transformation of variables presented the goodness of fit for Chl-*a* models (Harma *et al*. 2001, Kloiber *et al*. 2002). This method complicates the comparison of different models by means of the determination of coefficients, but the R^2 makes a slight improvement (figure 3) at 5–6% higher than those of the above-mentioned ratio at 700 nm and 670 nm. This approach has been proved to be successful in Lake Chagan shown as follows:

$$Y = 5.2715X + 2.0052 \quad (1)$$

where Y is logarithmic Chl-*a* and X refers to the logarithmic ratio of reflectance at 700 nm and at 670 nm.

3.4 *Assessment of Chl-a concentration in the lakes using TM data*

The broad bandwidth of TM data cannot spectrally resolve the prominent spectral features due to Chl-*a* absorption. The Chl-*a* absorption maximum at the red region of 670 or 680 nm is only half contained in the TM red band (630–690 nm), while the reflectance peak near 700 nm is totally out of the TM red region. So it is impossible to estimate Chl-*a* concentration from TM bands similarly to the use of field spectral regression method. This requires us to employ different methods that are applicable to TM data to determine Chl-*a*. Attempts were made to find single bands or band ratios of TM data. Previous investigations (Lathrop 1992, Lavery *et al*. 1993, Kloiber *et al*. 2002) suggested that band combinations such as ratios, multiplication and average provided useful relationships, and all were made using the averaged pixel digital numbers (DNs). In this study, a 3×3 pixel window corresponding to an area of 90×90 m was extracted from the images of each test site for water sampling data and field spectral measurements.

TM bands or their combinations were employed to estimate Chl-*a* as the following

$$Y = AX + B \quad (2)$$

where Y is Chl-*a*, and X is TM bands or their combinations.

3.5 *Trophic state index*

In this study, we applied Shu's modified model to estimate the trophic state index of the lakes. In Shu's method (1990), the modified algorithm for Chinese lakes' eutrophication assessment can be expressed as follows:

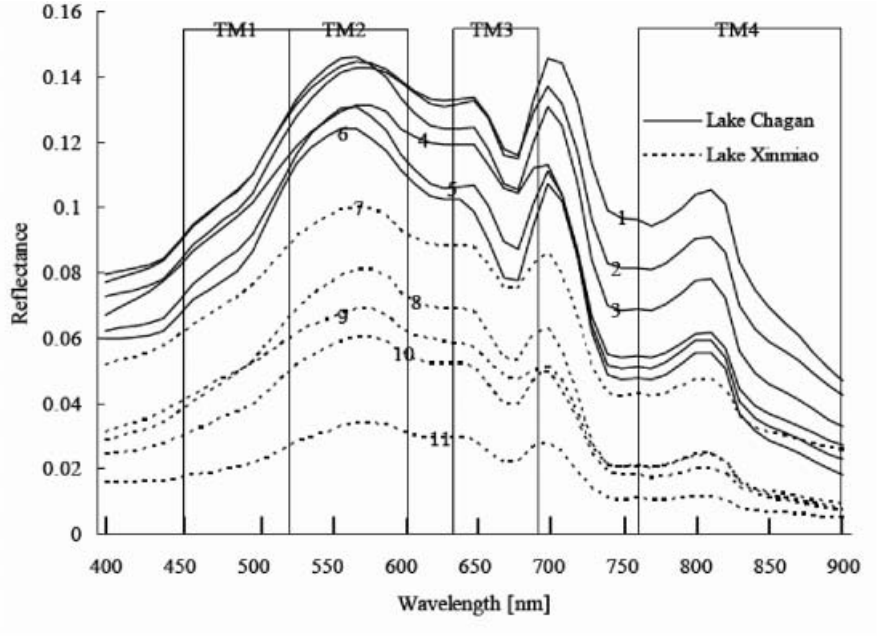

Notes: 1 is in October, 2 and 9 in May, 3 and 7 in August, 4 and 11 in June, 5 and 8 in September, 6 and 10 in July, and its corresponding Chl-*a* concentrations can be seen in Table 1 and Table 2.

Figure 2. Reflectance spectra in Lake Chagan and Lake Xinmiao: the upper five lines are for Lake Chagan and the bottom five lines are for Lake Xinmiao.

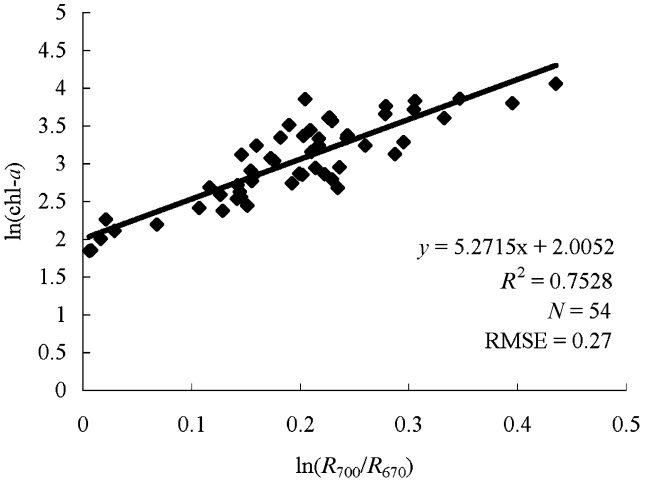

Figure 3. Correlation between logarithmic ratio of reflectance and Chl-*a* concentration in Lake Chagan.

$$\mathrm{TSI_M(chla)} = 10\left(2.46 + \frac{\ln(\mathrm{chla})}{\ln(2.5)}\right) \quad (3)$$

where chla means Chl-*a* concentration (μg/L).

Table 6 shows the assessment standards for each indicator based on the parameters used in evaluation of the eutrophication for Chinese lakes (Shu 1993).

4. Results and discussion

Lake Chagan is one of the eutrophic lakes in China with a high level of Chl-*a* and a low level of Secchi disk transparency (SDT): chl-*a* changes between 6 and 60 μg/L and Secchi disk ranges from 0.10 to 0.50 m (see table 1). In comparison, Lake Xinmiao as an oligo-mesotrophic lake shows Chl-*a* ranging from 0.35 to 44.48 μg/L and Secchi disk ranging from 0.23 to 0.96 m (see table 2). Lake Kuli varyies between the other two lakes with respect to Chl-*a* levels.

4.1 *Spectral characteristics of Chl-a concentration*

Figure 2 shows the reflectance spectra of Lake Chagan and Lake Xinmiao in different months with differing Chl-*a* concentration levels. They are common for inland water bodies with different trophic states. The resultant spectrum reveals a low reflectance value at the wavelength range 400–440 nm, which is because of absorption by both algal pigments (Chl-*a*) and dissolved organic matter (Gitelson *et al*. 1993). Between 440 and 550 nm, all values of spectral reflectance show a linear increase. At around 550–560 nm, there is an obvious reflectance peak, which is the result of low absorption by phytoplankton pigments, coupled with an increasing backscattering when the particle concentration increases. However, there are two reflectance minima near 630 and 670 nm. They both correspond to the absorption maximum of phytoplankton pigments (Gitelson and Kondratyev 1991). A small reflectance peak at around 650 nm can be observed, but a notable reflectance maximum exists at 690 nm because of fluorescence by Chl-*a* pigments (Gordon 1979). This fluorescence reflectance peak always has a shift towards longer wavelengths (Gitelson *et al*. 1993) in productive mesotrophic and eutrophic areas as Chl-*a* increases. The peak is at 700 nm due to the higher Chl-*a* levels in Lake Chagan and Lake Xinmiao. After 700 nm, all reflectance values drop quickly until 740 nm, and then they become very flat between 740 and 790 nm. There is a small but visible reflectance peak at 810 nm. Then these reflectance values slowly decrease until they are flat again from 840 to 900 nm. Therefore, it should be highlighted that such unique spectral characteristics of Chl-*a* exist in the lakes of the study area, but are

Table 6. Criteria for the lake's eutrophication assessment in the Chagan region.

Trophic state	$\mathrm{TSI_M}$ (Shu)	Chl-*a* content (μg/l)
Oligotrophic	$\leqslant 20$	$\leqslant 1.0$
Lower-mesotrophic	$\leqslant 30$	$\leqslant 2.0$
Mesotrophic	$\leqslant 40$	$\leqslant 4.0$
Upper-mesotrophic	$\leqslant 50$	$\leqslant 10.0$
Eutrophic	$\leqslant 70$	$\leqslant 65.0$
Hypereutrophic	$\leqslant 80$	$\leqslant 160.0$
Extremely hypereutrophic	$\leqslant 100$	$\leqslant 1000.0$

generally similar to those of reported lakes with similar trophic states (Arenz *et al.* 1996). All spectra shown in figure 2 were also regarded as a basis for the evaluation of lake trophic state using remote sensing observations in our study.

4.2 *Chl-a from field spectral and TM data*

Lake Chagan (Table 1) always presents a low-intermediate Chl-*a* level between 6 μg/L and 20 μg/L from May to June, the highest Chl-*a* level from 28 to 58 μg/L in July, a higher level of Chl-*a* concentration of 11–47 μg/L from August to September, and an intermediate Chl-*a* level of 10–28 μg/L in October 2004, respectively. Tables 3–5 show the Chl-*a* determination from field spectra for Lake Chagan and Lake Xinmiao that were investigated from May to October 2004. The result from field spectra in Lake Chagan gave a high correlation with the laboratory reference data (R^2=0.70) (see table 3). Here R^2 refers to the determination of coefficients.

In contrast, Lake Xinmiao (table 2) had a lowest Chl-*a* level between 0.30 μg/L and 1.30 μg/L in May 2004. There was a low-intermediate level of Chl-*a* concentration from 4 μg/L and 26 μg/L in June, a higher Chl-*a* level of 5–40 μg/L existed in July, an intermediate Chl-*a* level at 12–27 μg/L from August to September, and a low Chl-*a* level of 6–11 μg/L in October 2004, respectively. Chl-*a* derived from the field spectra in Lake Xinmiao had the best fit with *in situ* data (R^2=0.72 in table 4). In short, a large Chl-*a* range between 1 and 60 μg/L can be estimated from field spectra from May to October 2004 for both lakes with R^2=0.71 (table 5).

Applying equation (2), table 7 shows a good regression between Chl-*a* from TM data and Chl-*a* measurements in the laboratory, which presents R^2=0.63 for the two

Table 7. TM bands 1–4 and their combinations in correlation with Chl-*a* content represented in correlation coefficient (R^2) on 26 July 2004.

Variables	R^2 (Both Lakes)	R^2 (Chagan)	R^2 (Xinmiao)	Variables	R^2 (Both Lakes)	R^2 (Chagan)	R^2 (Xinmiao)
TM1	0.34	0.15	0.65	A.V.(1,2,3)	0.34	0.01	0.68
TM2	0.33	0.001	0.68	A.V.(1,2,4)	0.34	0.05	0.61
TM3	0.33	0.23	0.69	A.V.(2,3,4)	0.33	0.12	0.63
TM4	0.31	0.001	0.42	A.V.(1,3,4)	0.34	0.02	0.62
TM4/TM1	0.09	0.06	0.08	A.V.(1,2,3,4)	0.34	0.01	0.64
TM4/TM2	0.57	0.001	0.73	TM1*TM2	0.28	0.03	0.57
TM4/TM3	0.01	0.09	0.19	TM1*TM3	0.29	0.02	0.59
TM3/TM2	**0.63**	0.20	**0.88**	TM1*TM4	0.29	0.04	0.46
TM3/TM1	0.19	**0.38**	0.81	TM2*TM3	0.26	0.08	0.54
TM2/TM1	0.45	0.30	0.80	TM2*TM4	0.27	0.001	0.47
A.V.(3,4)	0.33	0.19	0.61	TM3*TM4	0.27	0.13	0.47
A.V. (2,4)	0.33	0.001	0.57	TM1*TM1	0.30	0.14	0.59
A.V.(1,4)	0.34	0.09	0.57	TM2*TM2	0.25	0.001	0.46
A.V.(3,2)	0.34	0.14	0.68	TM3*TM3	0.26	0.23	0.58
A.V.(3,1)	0.34	0.02	0.67	TM4*TM4	0.27	0.003	0.36
A.V.(2,1)	0.34	0.06	0.67				

Note: A.V. means average.

Table 8. TM bands 1–4 and their combinations in correlation with Chl-*a* content represented in correlation coefficient (R^2) on 14 October 2004.

Variables	R^2 (Both Lakes)	R^2 (Chagan)	R^2 (Xinmiao)	Variables	R^2 (Both Lakes)	R^2 (Chagan)	R^2 (Xinmiao)
TM1	0.78	0.27	**0.62**	A.V.(1,2,3)	0.78	0.31	0.12
TM2	0.78	0.38	0.49	A.V.(1,2,4)	0.83	0.53	0.32
TM3	0.76	0.16	0.01	A.V.(2,3,4)	0.81	0.47	0.32
TM4	0.87	0.62	0.47	A.V.(1,3,4)	0.81	0.47	0.30
TM4/TM1	0.85	0.41	0.50	A.V.(1,2,3,4)	0.81	0.46	0.25
TM4/TM2	0.09	0.26	0.49	TM1*TM2	0.82	0.37	0.53
TM4/TM3	**0.89**	**0.66**	0.51	TM1*TM3	0.80	0.26	0.08
TM3/TM2	0.12	0.43	0.35	TM1*TM4	0.88	0.57	0.44
TM3/TM1	0.34	0.11	0.36	TM2*TM3	0.82	0.32	0.53
TM2/TM1	0.66	0.14	0.45	TM2*TM4	0.87	0.56	0.34
A.V.(3,4)	0.82	0.48	0.37	TM3*TM4	0.86	0.52	0.45
A.V. (2,4)	0.84	0.59	0.41	TM1*TM1	0.80	0.26	0.62
A.V.(1,4)	0.84	0.56	0.38	TM2*TM2	0.85	0.38	0.59
A.V.(3,2)	0.77	0.26	0.01	TM3*TM3	0.78	0.16	0.03
A.V.(3,1)	0.77	0.27	0.05	TM4*TM4	0.89	0.62	0.48
A.V.(2,1)	0.78	0.35	0.58				

Note: A.V. means average.

lakes in July 2004. Chl-*a* was high from TM data in Lake Xinmiao in July 2004 with R^2=0.88. We also found that Chl-*a* for the two lakes was best estimated from TM data in October 2004 with R^2=0.89 (table 8 from equation (2)). Table 9 from

Table 9. TM bands 1–4 and their combinations in correlation with Chl-*a* content represented in correlation coefficient (R^2) for three lakes on 13 July 2005.

Variables	R^2	Variables	R^2
TM1	0.30	A.V.(1,2,3)	0.48
TM2	0.61	A.V.(1,2,4)	0.71
TM3	0.49	A.V.(2,3,4)	**0.72**
TM4	0.48	A.V.(1,3,4)	0.68
TM4/TM1	0.25	A.V.(1,2,3,4)	0.68
TM4/TM2	0.08	TM1*TM2	0.52
TM4/TM3	0.06	TM1*TM3	0.42
TM3/TM2	0.004	TM1*TM4	0.63
TM3/TM1	0.54	TM2*TM3	0.56
TM2/TM1	0.49	TM2*TM4	0.65
A.V.(3,4)	0.69	TM3*TM4	0.67
A.V. (2,4)	0.65	TM1*TM1	0.29
A.V.(1,4)	0.68	TM2*TM2	0.61
A.V.(3,2)	0.56	TM3*TM3	0.48
A.V.(3,1)	0.41	TM4*TM4	0.47
A.V.(2,1)	0.46		

Note: A.V. means average.

equation (2) indicates that TM data in July 2005 can be used to retrieve Chl-*a* with $R^2=0.72$ for the three lakes.

Lake Xinmaio, crowded with aquatic plants, has a good water quality condition. This is because its water supply from Songhua River through a canal first flows into Lake Xinmiao from its southern corner, and then runs into Lake Chagan and finally out of Lake Chagan. Therefore, Lake Chagan has a poor water quality condition because of its larger area and shallow depth with its loose mud bed easily floating off on windy days. Generally, during the same season in different years, Lake Chagan has a higher Chl-*a* level, but Lake Xinmiao at a lower Chl-*a* level and Lake Kuli varying between the two. Using equation (2), figure 4(*a*) shows that the Chl-*a* level ranged from 40 to 50 μg/L in Lake Chagan in July 2004. Since the water of Lake Xinmiao runs into Lake Chagan through an inlet from the south, the Chl-*a* level in the southern entrance of Lake Changan was between 30 and 40 μg/L. But the Chl-*a* level in Lake Xinmiao increased gradually from the south at 20–30 μg/L to its northern bank up to the level of 40–50 μg/L. Lake Kuli as an isolate lake had a Chl-*a* level of 30–40 μg/L in general.

From figure 4(*c*) using equation (2), we found that in general the Chl-*a* levels of three lakes in July 2005 were clearly lower than those of the three lakes in July 2004 (figure 4(*a*)). In July 2005, Chl-*a* levels in Lake Chagan were classified into four classes: a smaller area in its southern entrance at the Chl-*a* level of 10–30 μg/L, a major central part at the Chl-*a* level of 30–40 μg/L, some edge areas at 40–60 μg/L,

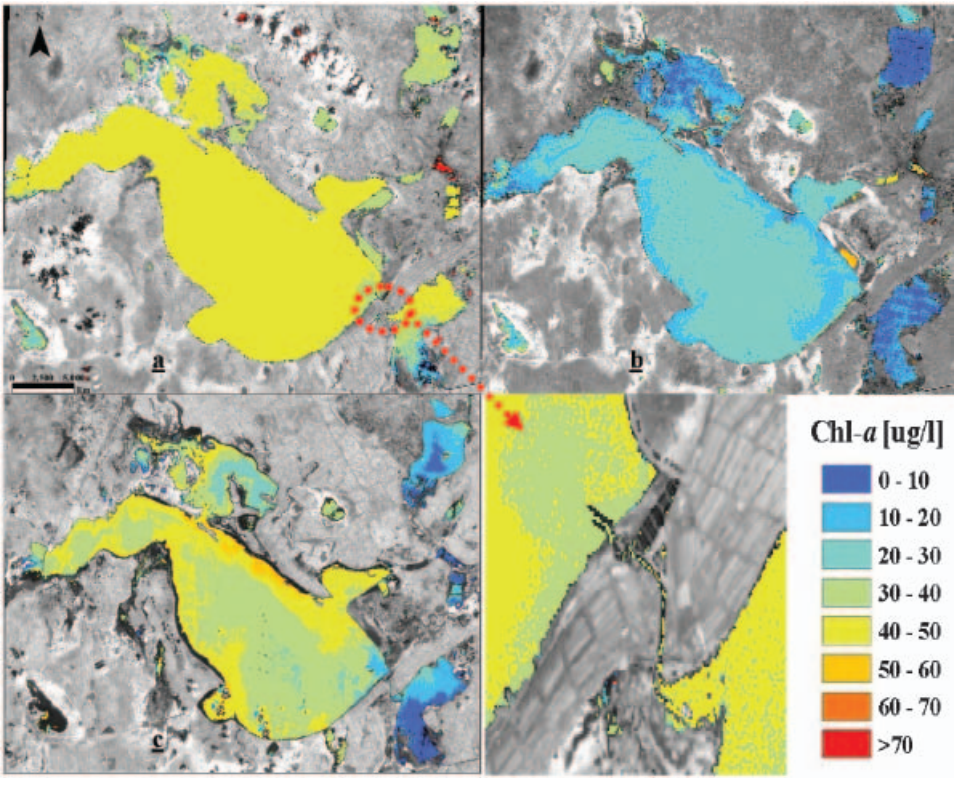

Figure 4. Chl-*a* levels estimated from the TM data: (a) on 26 July 2004; (b) on 14 October 2004; (c) on 13 July 2005.

and small northern areas at the level of 20–40 μg/L. In comparison, Lake Xinmiao was divided into three classes from its south to its north: 0–10, 10–20 and 20–30 μg/L. Similarly, Lake Kuli was also divided into three classes from the inside to the outside: 0–10, 10–20 and 20–30 μg/L. In addition, it is obvious that Chl-*a* levels were lower in October 2004 (figure 4(*b*)) than those in July 2004 (figure 4(*a*)). We observed that the lowest Chl-*a* level at 0–20 μg/L was distributed in the major part of Lakes Xinmiao and Kuli and in several minor areas around the Lake Chagan edge, while the majority of Lake Chagan had a Chl-*a* level of 20–30 μg/L in October 2004.

By comparing the Chl-*a* levels of the three lakes in July with those in October of both 2004 and 2005, we found that the Chl-*a* concentration level in the summer was much greater than that in the late autumn during the yearly cycle. This probably means that these lakes in our study area always exist in algal blooms in July, but the Chl-*a* levels decrease in the wake of the air temperature becoming lower and lower from August to October. Additionally, even in the same season (e.g., in the summer) of different years, we noted that the general Chl-*a* level in July 2005 was lower than that in July 2004. This is because of the fact that the summer season of 2005 had lower air temperatures, more rainfall and more water supply than those of the same season of 2004 over the lakes' region. Therefore, long-term observation is required to verify such a changing trend of Chl-*a* concentration in the lakes in our future studies.

4.3 *Trophic state analysis from field spectra and TM data*

Figure 5 indicates the results of the trophic state index modified (TSI_M) calculated from Chl-*a* estimate using field spectra and those of TSI_M derived from Chl-*a* values measured in the laboratory for both Lake Chagan and Lake Xinmiao. Here the TSI_M obtained from spectral data excluded Lake Kuli due to no field spectral measurements in Lake Kuli in our datasets. All data for the two lakes from May to October 2004 gave expected results, and their average level and general seasonal variation were also reasonably represented. The comparison of these results shows that the accuracy is satisfactory in the study. Figure 6(*a*) gives a high correlation of TSI_M determined from field spectra with TSI_M from laboratory reference data with R^2 of 0.71 and RMSE of 9.74 μg/L in Lake Chagan, and a similar correlation with R^2 of 0.65 and RMSE of 12.88 μg/L in Lake Xinmiao (figure 6(*b*)).

Figure 5(*a*) demonstrates that TSI_M increased as the Chl-*a* level increased in the wake of the air temperature becoming warmer and warmer from May to July 2004. During the summer, Chl-*a* levels were apparently increasing and TSI_M was also at the maximum in July so that few small pieces were characterised as the hyper-eutrophic state. On the other hand, TSI_M decreased when Chl-*a* levels dropped along with the air temperature getting lower and lower from August to October 2004. As a result, TSI_M in October became the lowest in our datasets. According to the indictor of TSI_M in the year of 2004, Lake Chagan was mostly in the eutrophic state, except in a few small areas which were in the upper-mesotrophic state in May and June, while some small parts were in the hypereutrophic state in July. This implied that most of Lake Chagan was attributed to the eutrophic state in 2004 when Chl-*a* levels were also being considered (figure 5(*a*)). A similar change trend of the trophic state in Lake Xinmiao is given in figure 5(*b*), but the lower level of the trophic states existed especially in May 2004 as oligotrophic and lower-mesotrophic states, due to its better water quality condition in Lake Xinmiao.

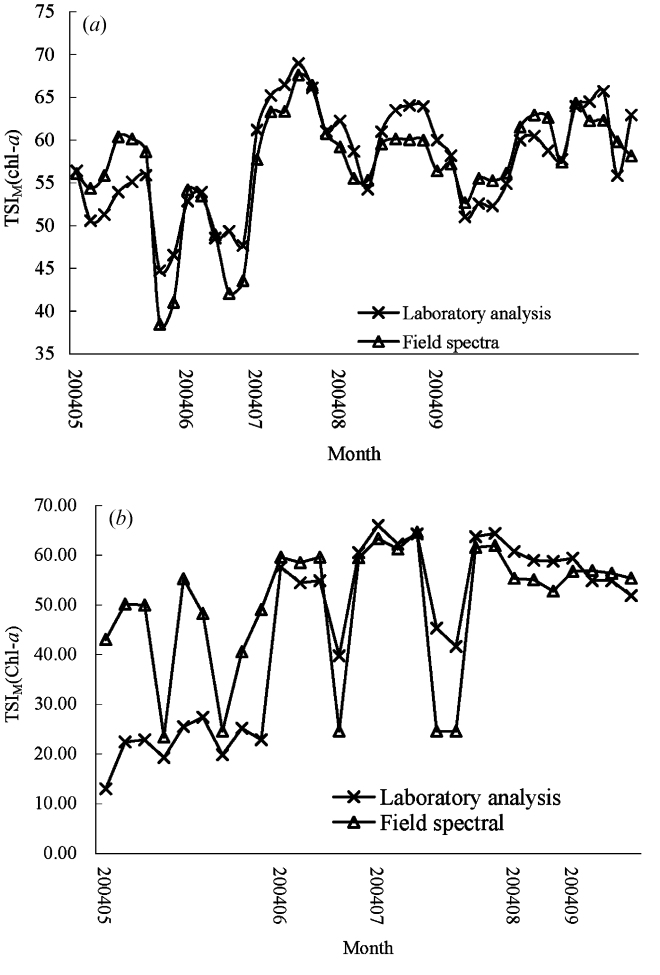

Figure 5. Trophic state index derived from the laboratory analysis and field spectra: (a) Lake Chagan; (b) Lake Xinmiao.

Applying equation (3), figures 7(*a*)–(*c*) and 8(*a*)–(*c*) are the distribution maps of TSI_M values and trophic states derived from TM data corresponding to three dates collected in 2004 and 2005, respectively. Figure 7(*a*) shows that three lakes have TSI_M values between 60 and 70, except the southern area of Lake Xinmiao at the low level of 50–60. Thus, all areas of three lakes were classified as the eutrophic state on 26 July 2004 (figure 8(*a*)).

We observed that the Chl-*a* level was lower in July 2005 than in July 2004, which mainly resulted from lower temperatures, more rainfall and more water supplies in the summer season of 2005 over the northwest Jilin Province. However, most of Lake Chagan was still at the same level of TSI_M from 60 to 70 in July 2005 as in July 2004, while a small southern area existed at the level of 50–60 (Figure 7(*c*)). In contrast, Lake Xinmiao and Kuli showed lower levels of TSI_M values in July 2005 than in July 2004. As its levels of TSI_M ranged from 20 to 60 (Figure 7(*c*)), Lake Xinmiao was classified into three classes from the south to the north in July 2005, i.e., lower-mesotrophic, mesotrophic and upper-mesotrophic status (table 6 and figure 8(*c*)), respectively. Due to its TSI_M levels varying between Lake Chagan and

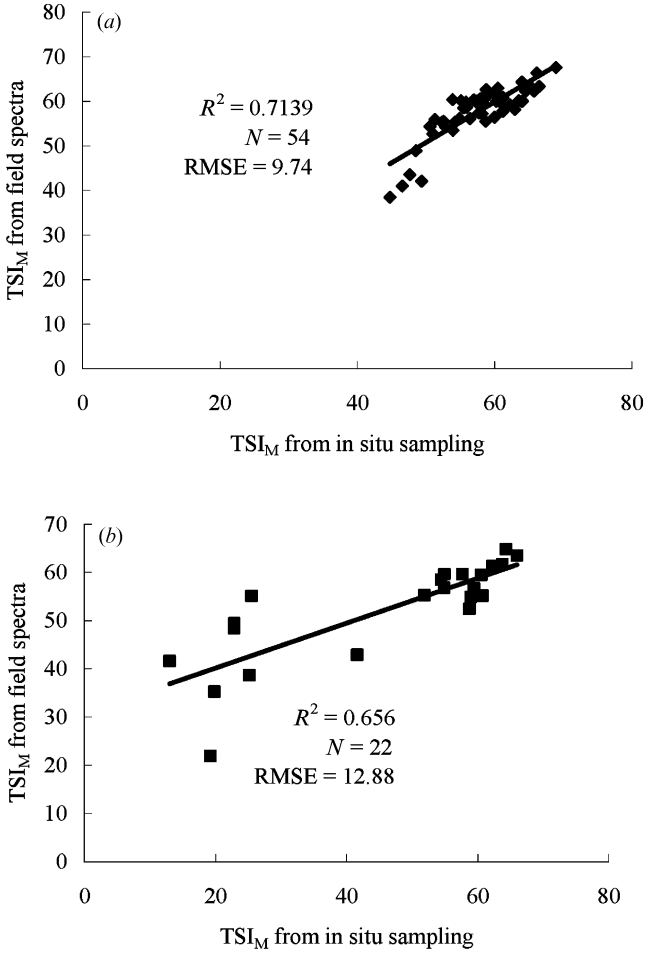

Figure 6. Correlation between TSI_M retrieved from *in situ* measurements and TSI_M from field spectra: (a) Lake Chagan; (b) Lake Xinmiao.

Lake Xinmiao, the majority of Lake Kuli was characterized as the eutrophic state at the TSI_M level of 50–60, while its minority in the central area was attributed to the upper-mesotrophic status at the level TSI_M of 40–50 (figure 7(*c*) and figure 8(*c*)).

Figure 7(*b*) and Figure 8(*b*) show TSI_M values and trophic states of three lakes on 14 October 2004. We noted that TSI_M values decreased from July to October, as the air temperature became lower and lower from July to October. It is clear that Lake Xinmiao and Kuli dropped to lower levels of trophic states in October than in July 2004, but Lake Chagan was still at the same eutrophic state in October (figure 8(*b*)) as in July 2004, even as in the case of TSI_M values at the lower level of 50–60 in October (figure 7(*b*)) than at the level of 60–70 in July 2004. According to TSI_M values (table 6) derived from the TM image in October 2004, the majority of Lake Chagan was classified as the eutrophic state, while few small pieces of the lake at 20–50 were classified as lower-mesotrophic, mesotrophic and upper-mesotrophic states, but none as the hypertrophic state. The spatial distribution of TSI_M values was almost the same as the distribution of Chl-*a* levels due to the similar factors. The highest level of TSI_M values between 60 and 70 was noted in the southern area of

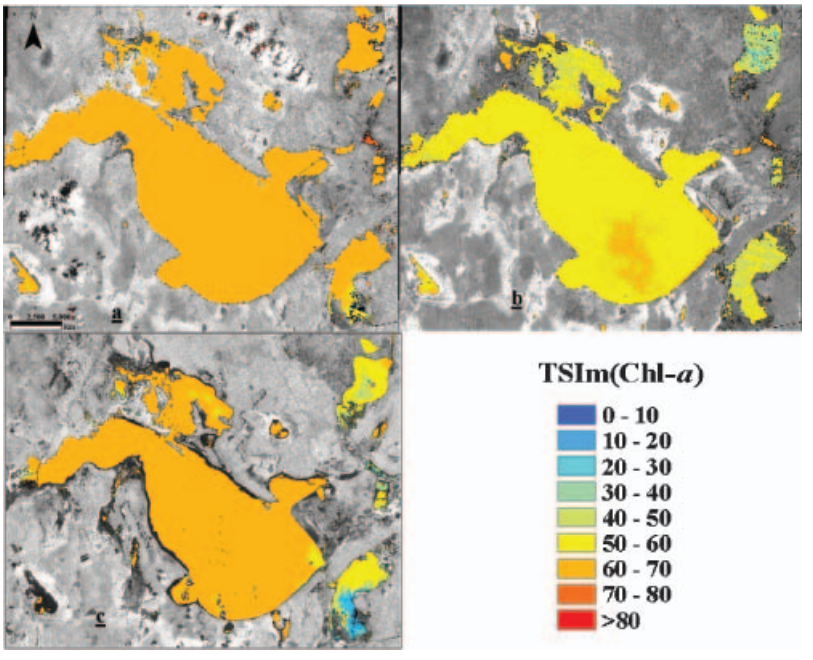

Figure 7. TSI_M(chl-*a*) nine classes determined from TM data: (a) on 26 July 2004; (b) on 14 October 2004; (c) on 13 July 2005.

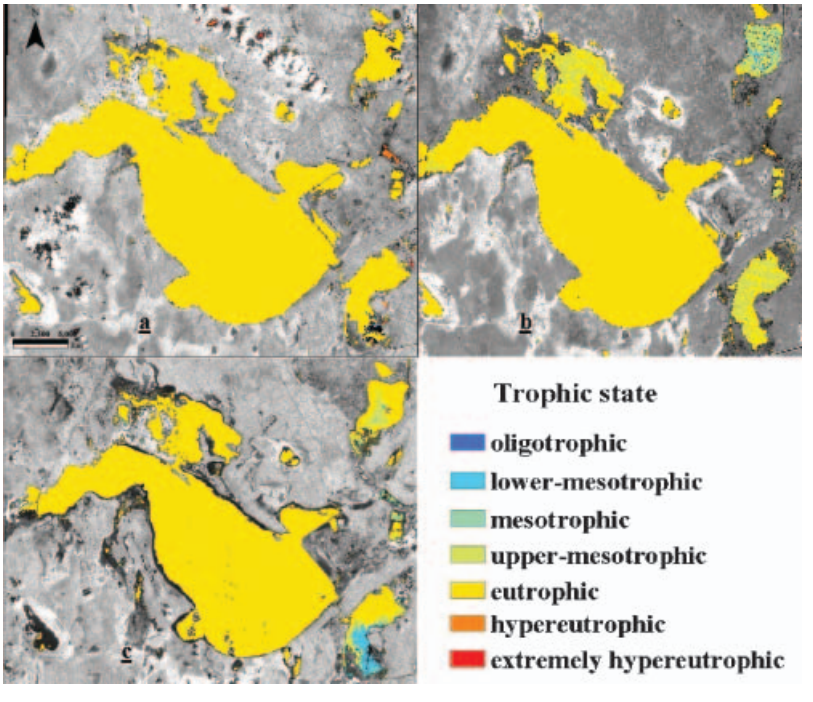

Figure 8. Trophic states of three lakes evaluated from TM data: (a) on 26 July 2004; (b) on 14 October 2004; (c) on 13 July 2005.

Lake Chagan, and higher TSI_M at the level of 50–60 could be seen in the majority of Lake Chagan and small areas in Lake Xinmiao and Lake Kuli as the eutrophic state. The intermediate TSI_M level of 40–50 mainly existed in Lake Xinmiao as the upper-mesotrophic state, while low TSI_M values in the range of 20–40 were mostly distributed in Lake Kuli (figure 7(*b*)) as lower-mesotrophic and mesotrophic states (figure 8(*b*)).

Figure 9(*a*)–(*d*) show accepted and reliable regression results between TSI_M from TM data and TSI_M from Chl-*a* data in the laboratory analysis with the lowest R^2 of 0.73 and the maximum RMSE of 8.96 μg/L for the three lakes. The results suggest that the approach of estimating Chl-*a* and trophic state index from space-borne measurements proves to be an appropriate method for the determination of lake trophic states in our study.

5. Conclusions

Space-borne remotely sensed data were applied to estimate Chl-*a* concentration and evaluate the eutrophication of three lakes in the northwest Jilin Province of Northeast China. We observed that Chl-*a* levels of the lakes in our study area were

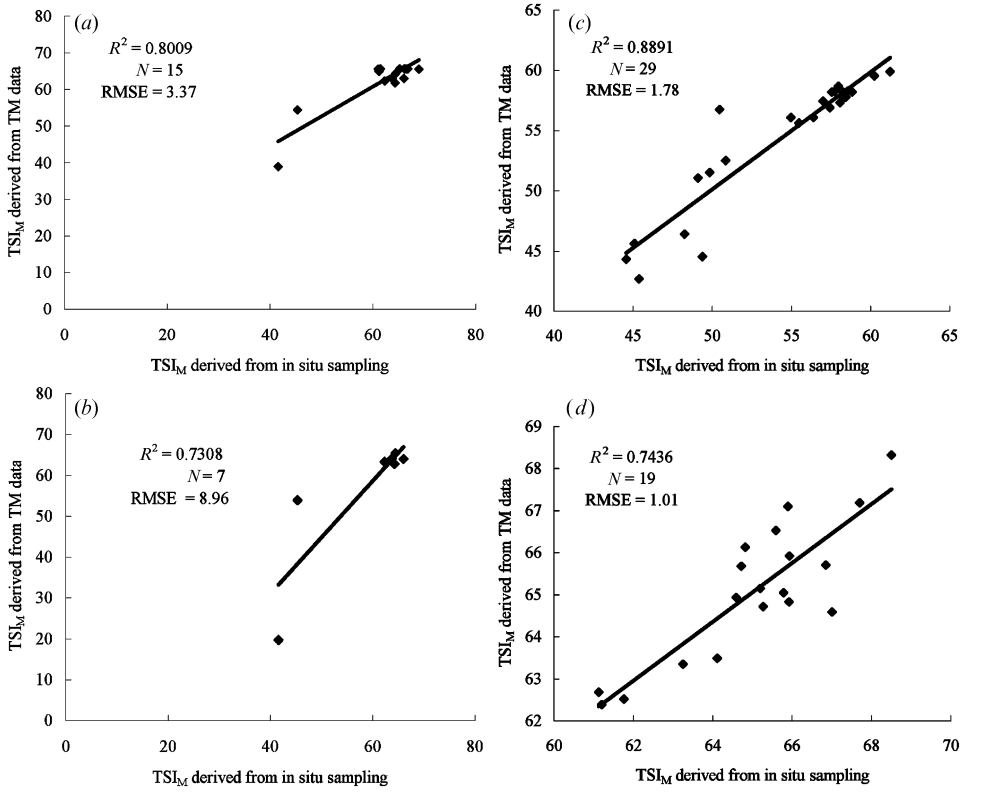

Figure 9. (a) Correlation between TSI_M derived from in situ Chl-*a* and from TM data in Lake Chagan on 26 July 2004. (b) Correlation between TSI_M estimated from in situ Chl-*a* and from TM data in Lake Xinmiao on 26 July 2004. (c) Correlation between TSI_M retrieved from *in situ* Chl-*a* and from TM data in Lake Chagan and Lake Xinmiao on 14 October 2004. (d) Correlation between TSI_M derived from in situ Chl-*a* and from TM data for three lakes on 13 July 2005.

low in May after the lake melting period in March–April. Then they increased rapidly in June and reached the highest Chl-*a* level in July. From August to October, Chl-*a* levels gradually became lower and lower until November when the lakes were frozen in the region. Our results show that Landsat TM data and field spectral measurements with similar Chl-*a* field data can be used effectively to determine the levels of Chl-*a* concentration and trophic state index for inland lakes in the study area. One advantage of using space-borne observations is the capability of their multi-temporal application with a large coverage and low costs compared to airborne-based measurements and laboratory analysis for the evaluation of the trophic states over several lakes.

The unique characteristics of field reflectance spectra in Lake Chagan and Lake Xinmiao are generally similar in shape to those from many other lakes with similar trophic states. Furthermore, the comparison of Chl-*a* retrieval from spectral measurements shows that their estimated results are relatively stable and reasonable. The obtained result also shows that the Chl-*a* logarithmic transformation can help improve the estimated accuracy, but limited at 5–6% higher than the reflectance ratio method using our two-year datasets.

Although Landsat TM has broad spectral bandwidths and its band limits encompass a mixture of spectrally opposing absorption and scattering features of chlorophyll-a or other photosynthetic pigments, it is still useful to develop consistent and reliable relationships between satellite-based observations and Chl-*a* concentration. The study demonstrates that Chl-*a* levels estimated from the TM bands and their band combinations provides an acceptable accuracy. The utility for such consistent combinations of TM data makes the analysis of their multi-temporal images comparable. This is a key step towards standardizing the approach. Our results indicate that Landsat TM data in different seasons of the year (e.g., July and October 2004) or in the same season of different years (e.g., July 2004 and July 2005) can provide reasonable results to estimate Chl-*a* levels when compared to the results obtained from field spectra measurements in the study.

We also compared Chl-*a* analysis in the laboratory with Chl-*a* levels determined from both field spectral observations and Landsat TM data. The estimated Chl-*a* results are reliable and acceptable with the determination coefficients equal to or greater than 0.70, as the basis of the trophic state evaluation for the lakes in our study. The study proves that the space-borne remote sensing approach is successful in the evaluation of lake trophic states in the northwest Jilin Province of Northeast China. Moreover, the results verify that the lake trophic states of the area agree with the other studies of traditional investigations. They outlined the need for long-term monitoring of water quality conditions for the lakes in the region.

Acknowledgements

The authors would like to acknowledge financial support from the Knowledge Innovation Program of the Northeast Institute of Geography and Agricultural Ecology (NEIGAE), Chinese Academy of Sciences (CAS), National Natural Science Foundation of China (NSFC) projects (40401003 and 40371082), and the Finnish Nessling Foundation. Yuanzhi Zhang's work was carried out partly at Laboratory of Space Technology, Helsinki University of Technology in Finland and partly at CARTEL, University of Sherbrooke, Canada. They also thank two anonymous reviewers' comments to improve the scientific quality of the original manuscript.

References

AHN, Y., SHANMUGAM, P. and MOON, J., 2006, Retrieval of ocean colour from high resolution multi-spectral imagery for monitoring highly dynamic ocean features. *International Journal of Remote Sensing*, **27**, pp. 367–392.

AIZAKI, M., IWAKUMA, T. and TAKAMURA, N., 1981, Application of modified Carlson's trophic state index to Japanese lakes and its relationship to other parameters related to trophic state. *Report of Special Research Project of the National Institute for Environmental Studies*, **23**, pp. 13–31.

ARENZ, R.F., LEWIS, W.M. and SAUNDERS, J.F., 1996, Determination of chlorophyll and dissolved organic carbon from reflectance data for Colorado reservoirs. *International Journal of Remote Sensing*, **17**, pp. 1547–1566.

BRIVIO, P.A., GIARDINO, C. and ZILIOLI, E., 2001, Validation of satellite data for quality assurance in lake monitoring applications. *Science of the Total Environment*, **268**, pp. 3–13.

CARLSON, R.E., 1977, A trophic state index for lakes. *Limnol. Oceanog.*, **22**, pp. 361–369.

CHEN, Q., ZHANG, Y., EKROOS, A. and HALLIKAINEN, M., 2004, The role of remote sensing technology in the EU Water Framework Directive (WFD). *Environmental Science and Policy*, **7**, pp. 267–276.

DEKKER, A.G., 1993, Detection of optical water parameters for eutrophic lakes by high resolution remote sensing. PhD Dissertation, Free University, Amsterdam.

DEKKER, A.G. and PETERS, S.W.M., 1993, The use of the Thematic Mapper for the analysis of eutrophic lakes: a case study in the Netherlands. *International Journal of Remote Sensing*, **14**, pp. 799–821.

ERKKILA, A. and KALLIOLA, R., 2004, Patterns and dynamics of coastal waters in multi-temporal satellite images: support to water quality monitoring in the Archipelago Sea, Finland. Estuarine. *Coastal and Shelf Science*, **60**, pp. 165–177.

GHULAM, A., QIN, Q., ZHU, L. and ABDRAHMAN, P., 2004, Satellite remote sensing of groundwater: quantitative modelling and uncertainty reduction using 6S atmospheric simulations. *International Journal of Remote Sensing*, **25**, pp. 5509–5524.

GIARDINO, C., PEPE, M., BRIVIO, P.A., GHEZZI, P. and ZILIOLI, E., 2001, Detecting chlorophyll, Secchi disk depth and surface temperature in a sub-alpine lake using Landsat imagery. *Science of the Total Environment*, **268**, pp. 19–29.

GITELSON, A.A., GARBUZOV, G., SZILAGYI, F., MITTENZWAY, K.H., KARNIELI, A. and KAISER, A., 1993, Quantitative remote sensing methods for real-time monitoring of I inland waters quality. *International Journal of Remote Sensing*, **14**, pp. 1269–1295.

GITELSON, A.A. and KONDRATYEV, K.Y., 1991, Optical models of mesotrophic and eutrophic water bodies. *International Journal of Remote Sensing*, **12**, pp. 373–385.

GORDON, H.R., 1979, Diffusive reflectance of the ocean: the theory of its augmentation by chlorophyll-a fluorescence at 685 nm. *Applied Optics*, **18**, pp. 1161–1166.

HARMA, P., VEPSALAINEN, J., HANNONEN, T., PYHALAHTI, T., KAMARI, J., KALLIO, K., ELOHEIMO, K. and KOPONEN, S., 2001, Detection of water quality using simulated satellite data and semi~empirical algorithms in Finland. *Science and the Total Environment*, **268**, pp. 107–121. http://www.asdi.com.

KALLIO, K., KUTSER, T., HANNONEN, T., KOPONEN, S., PULLIAINEN, J., VEPSALAINEN, J. and PYHALAHTI, T., 2001, Retrieval of water quality from airborne imaging spectrometry of various lake types in different seasons. *Science and the Total Environment*, **268**, pp. 59–77.

KLOIBER, S.M., BREZONIK, P.L., OLMANSON, L.G. and BAUER, M.E., 2002, A procedure for regional lake water clarity assessment using Landsat multispectral data. *Remote Sensing of Environment*, **82**, pp. 38–47.

KOPONEN, S., PULLIAINEN, J., KALLIO, K. and HALLIKAINEN, M., 2002, Lake water quality classification with airborne hyperspectral spectrometer and simulated MERIS data. *Remote Sensing Environment*, **79**, pp. 51–59.

KOPONEN, S., PULLIAINEN, J., SERVOMAA, H., ZHANG, Y., HALLIKAINEN, M., KALLIO, K., VEPSALAINEN, J., PYHALAHTI, T. and HANNONEN, T., 2001, Analysis on the feasibility

of multisource remote sensing observations for Chl-a monitoring in Finish lakes. *Science and the Total Environment*, **268**, pp. 95–106.

LATHROP, R.G., 1992, Landsat thematic mapper monitoring of turbid inland water quality. *Photogramming Engineering and Remote Sensing*, **58**, pp. 465–470.

LAVERY, P., PATTIARATCHI, C., WYLLIE, A. and HICK, P., 1993, Water quality monitoring in estuarine waters using the Landsat Thematic Mapper. *Remote Sensing of Environment*, **46**, pp. 268–280.

LEE, T. and KAUFMAN, Y., 1986, Non-Lambertian effects on remote-sensing of surface reflectance and vegetation index. *IEEE Transactions on Geoscience and Remote Sensing*, **24**, pp. 699–708.

OSTLUNDA, C., FLINKA, P., STROMBECKB, N., PIERSONB, D. and LINDELL, T., 2001, Mapping of the water quality of Lake Erken, Sweden, from Imaging Spectrometry and Landsat Thematic Mapper. *Science and the Total Environment*, **268**, pp. 139–154.

PORCELLA, D.B., PETERSON, S.A. and LARSEN, D.P., 1980, Index to evaluate lake restoration. *J. Environ. Eng. Div. ASCE*, **106**, pp. 1151–1169.

PULLIAINEN, J., KALLIO, K., ELOHEIMO, K., KOPONEN, S., SERVOMAA, H., HANNONEN, T., TAURIAINEN, S. and HALLIKAINEN, M., 2001, A semi-operative approach to lake water quality retrieval from remote sensing data. *Science and the Total Environment*, **268**, pp. 79–93.

RITCHIE, J.C., COOPER, C.M. and SCHIEBE, F.R., 1990, The relationship of MSS and TM digital data with suspended sediments, chlorophyll, and temperature in Moon Lake, Mississippi. *Remote Sensing of Environment*, **33**, pp. 137–148.

SCHALLES, J., GITELSON, A., YACOBI, Y. and KROENKE, A., 1998, Estimation of chlorophyll-a from time series measurements of high spectral resolution reflectance in an eutrophic lake. *Journal of Phycology*, **34**, pp. 383–390.

SHU, J.H., 1990, Discussion of assessment methods of eutrophication in main lakes of China. *Environmental pollutions and control*, **12**, pp. 2–7 (in Chinese).

SHU, J.H., 1993, Assessment of eutrophication in main lakes of China. *Oceanologia and Limnologia Sinica*, **24**, pp. 616–620 (in Chinese).

THIEMANN, S. and KAUFMANN, H., 2000, Determination of Chlorophyll Content and Trophic State of Lakes Using Field Spectrometer and IRS-1C Satellite Data in the Mecklenburg Lake District, Germany. *Remote Sensing of Environment*, **73**, pp. 227–235.

WALKER, W.W., 1979, Use of hypolimnetic oxygen depletion rate as a trophic state index for lakes. *Water Res*, **15**, pp. 1463–1470.

WANG, Y.P., XIA, H., FU, J. and SHENG, G.Y., 2004, Water quality change in reservoirs of Shenzhen, China: detection using LANDSAT/TM data. *Science and the Total Environment*, **328**, pp. 195–206.

XING, K.X., GUO, H.C., SUN, Y.F. and HUANG, Y.T., 2005, Assessment of the spatial-temporal eutrophic character in the Lake Dianchi. *Journal of Geographical Sciences*, **15**, pp. 37–43.

XU, F.L., SHU, T., DAWSON, R.W. and LI, B.G., 2001, A GIS-based method of lake eutrophication assessment. *Ecological Modelling*, **144**, pp. 231–244.

ZHANG, Y., KOPONEN, S., PULLIAINEN, J. and HALLIKAINEN, M., 2002, Application of an empirical neural network to surface water quality estimation in the Gulf of Finland using combined optical data and microwave data. *Remote Sensing of Environment*, **81**, pp. 327–336.

ZHANG, Y., KOPONEN, S., PULLIAINEN, J. and HALLIKAINEN, M., 2003a, Application of empirical neural networks to chlorophyll-a estimation in coastal waters using remote optosensors. *IEEE Sensors Journal*, **3**, pp. 376–382.

ZHANG, Y., KOPONEN, S., PULLIAINEN, J. and HALLIKAINEN, M., 2003b, Water quality retrievals from combined Landsat TM and ERS-2 SAR data in the Gulf of Finland. *IEEE Transactions on Geoscience and Remote Sensing*, **41**, pp. 622–629.

ZHANG, Y., KOPONEN, S., PULLIAINEN, J. and HALLIKAINEN, M., 2003c, Empirical algorithms for Secchi disk depth using optical and microwave remote sensing data from the Gulf of Finland and the Archipelago Sea. *Boreal Environment Research*, **8**, pp. 251–261.